Article

Second-Order Predefined-Time Terminal Sliding Mode Control for Speed Regulation System of Permanent Magnet Synchronous Motor

Haibo Xue and Xinghua Liu *

School of Mechanical Engineering, Beijing Institute of Technology, Beijing 100081, China
* Correspondence: lxh@bit.edu.cn

Abstract: In this paper, a second-order predefined-time terminal sliding mode (SPTSM) is proposed, which is investigated for the practical applications of the speed regulation system of a permanent magnet synchronous motor (PMSM) by using predefined-time stability theory and Lyapunov stability theory. At first, we propose the SPTSM, which involves the controller's design by using the novel reaching law with predefined-time terminal sliding mode (PTSM) and the novel sliding mode surface with PTSM. Second, we derive the novel SPTSM controller for the universal second-order nonlinear single-input single-output (SISO) system and the practical applications of the speed regulation system of the PMSM separately. Then, numerical simulation results of the speed regulation system of the PMSM are also included to check the effect of the theoretical results and the corresponding parameters on the convergence rates, so that the results can be guidance for the selection of SPTSM controller parameters. Finally, the dynamic responsiveness and robustness of the system are validated through numerical simulations and experimental results. It has been observed that the robust SPTSM controller, which is designed with the PTSM-PTSM, referring to the sliding mode that involves a reaching law with PTSM and a sliding mode surface with PTSM, exhibits superior performance.

Keywords: permanent magnet synchronous motor (PMSM); predefined-time terminal sliding mode (PTSM); second-order predefined-time terminal sliding mode (SPTSM); speed regulation system; nonlinear system

1. Introduction

A permanent magnet synchronous motor (PMSM) control system is a kind of typical nonlinear time-varying system [1–4]. High tracking accuracy, efficient dynamic response, and strong robustness are considered as the main objects of PMSM control system design [5,6]. So, some nonlinear system control methods are usually used in PMSM control systems, which improve the control performance of PMSMs in different aspects based on their advantages [7,8]. Among them, sliding mode control (SMC) has been widely used in PMSMs and other nonlinear control systems because of its simple control system, excellent dynamic response, and insensitivity to parameter disturbance and external disturbance [9,10]. Its effectiveness has also been experimentally verified. It improves the robustness of the system to the PMSM drive system with load disturbance and parameter uncertainty, and can improve the control accuracy and response speed in the control system of a PMSM [4,11,12].

Based on the theories of SMC, several representative reaching laws have been proposed, including the constant reaching law, exponential reaching law, power reaching

law, and general reaching law, all of which aim to achieve faster convergence rates [13,14]. These SMC laws all have discontinuous sign functions, which will inevitably cause the chattering problem, and also easily affect the performance of the control system [15,16]. In addition, the issue of chattering and the system's convergence rate form a pair of mutually limiting contradictions that cannot be entirely eliminated, but can only be alleviated to a certain extent [17]. The control problem can be reframed as a suitable approximate linear–quadratic problem. Here, the coupling parameters are determined by the Riccati equation [18–20]. To improve the reaching quality of SMC, terminal sliding mode control (TSM) is proposed [21–23]. By introducing terminal attractors, TSM has no switching function in the control system and effectively eliminates the chattering problem in the convergence process [23], but it does not achieve the optimal convergence rate. However, the fast terminal sliding mode (FTSM) is proposed to improve the convergence rate [24].

For control systems, the settling time is commonly used as a criterion to evaluate the quality of the control system. Based on the settling time characteristics, control systems can be categorized into three types: finite-time control [25–27], fixed-time control [14,28–30], and predefined-time control [31–35]. Among them, the predefined-time terminal sliding mode (PTSM) combines the advantages of both predefined time and TSM, serving as the amalgamation, and its total settling time T_c for the system is determined by the predefined-time parameter T_p, i.e., $T_c(x_0) \leq T_p$. Therefore, it has garnered widespread attention, particularly in the realm of nonlinear control systems, where extensive research has been conducted [33,35–37].

Motivated by the aforementioned discussion, we delve into the investigation of the novel second-order predefined-time terminal sliding mode (SPTSM) controllers. These controllers are dedicated to the conception and actualization of the integration of high-order SMC strategies, predefined-time control, and fractional computation for second-order nonlinear single-input single-output (SISO) systems. First, based on predefined-time synchronization theory and Lyapunov stability theory, we propose the SPTSM, which involves the controller's design by using the novel reaching law with PTSM and the novel sliding mode surface with PTSM for a second-order nonlinear SISO system. Second, we derive the novel SPTSM controller for the universal second-order nonlinear SISO system and the practical applications of the speed regulation system of a PMSM separately. Third, the controllers and their respective parameters are meticulously designed and comprehensively investigated for comparison. Then, the effectiveness of the SPTSM controllers is validated through numerical simulations. Finally, an experiment platform for PMSM drive control is established to verify the dynamic response and robustness of the speed regulation system under the novel sliding modes.

The remainder of this article is organized as outlined below. In Section 2, we derive the second-order state equation of the speed regulation system of a PMSM. Then, the fundamental definitions and lemmas are included, and several novel theories, which involve the SPTSM controllers for a second-order nonlinear SISO system, are proposed in Section 3. The results of simulations and experiments are given in Section 4 to demonstrate the dynamic response and robustness of the SPTSM controller. Section 5 provides a conclusive overview and poses open problems for further exploration.

2. Mathematical Model

2.1. Mathematical Model of PMSM

An ideal PMSM neglects saturation of the motor core and neglects eddy currents and hysteresis losses. The mathematical model of a PMSM on the $d - q$ axis can be formulated as follows [38].

$$L_d \frac{di_d}{dt} = -Ri_d + P_n \omega_m L_q i_q + u_d \tag{1}$$

$$L_q \frac{di_q}{dt} = -Ri_q - P_n \omega_m L_d i_d - P_n \omega_m \psi_f + u_q \tag{2}$$

$$J\frac{d\omega_m}{dt} = -B\omega_m + T_e - T_L \tag{3}$$

$$T_e = \frac{3}{2} P_n i_q \left(i_d (L_d - L_q) + \psi_f \right) \tag{4}$$

where R is the stator resistance; P_n is the number of pole pairs; ω_m is the angular velocity; ψ_f is the rotor flux linkage; T_L is the load torque; B is the viscous frictional coefficient; J is the rotor inertia; L_d, L_q are the d-axis and q-axis stator inductance; u_d, u_q are the d-axis and q-axis stator voltage, respectively; and i_d, i_q are the d-axis and q-axis stator current, respectively.

In this paper, we consider a surface PMSM as an example,

$$L_d = L_q = L \tag{5}$$

where L is the stator inductance.

Equations (3) and (4) can be rewritten as follows.

$$T_e = \frac{3}{2} P_n \psi_f i_q \tag{6}$$

$$\frac{d\omega_m}{dt} = \frac{1}{J} \left(\frac{3}{2} P_n \psi_f i_q - B\omega_m - T_L \right) \tag{7}$$

2.2. Second-Order State Equation

Based on Equation (7), we define the state variables of the speed error for a PMSM speed regulation system as follows.

$$x_1 = \omega_{ref} - \omega_m \tag{8}$$

where ω_{ref} is the reference spee, which is a positive constant, and ω_m is the actual speed of the PMSM.

Here, we assume that T_L is a constant or a quasi-static parameter with a rate of change significantly smaller than that of the angular velocity of the PMSM.

The derivative of x_1 is defined as x_2, and the derivatives of x_1, x_2 are, respectively, expressed as follows.

$$\begin{cases} \dot{x}_1 = -\frac{1}{J}\left(\frac{3}{2} P_n \psi_f i_{qref} - B\omega_m - T_L \right) \\ \dot{x}_2 = -\frac{1}{J}\left(\frac{3}{2} P_n \psi_f \frac{di_{qref}}{dt} - B\frac{d\omega_m}{dt} \right) \end{cases} \tag{9}$$

The second-order state equation of the speed regulation system of the PMSM can be obtained as follows.

$$\begin{cases} \dot{x}_1 = x_2 \\ \dot{x}_2 = -\frac{1}{J}\left(\frac{3}{2} P_n \psi_f u - B\frac{d\omega_m}{dt} \right) \end{cases} \tag{10}$$

where $u = di_{qref}/dt$.

3. Fractional Robust Control Design

This section delineates the evolution of an investigation that is dedicated to the conceiving and actualizing of an integration of high-order SMC strategies, predefined-time control, and fractional computation within the speed regulation system of a PMSM. Hence, a novel methodology, namely the SPTSM controller, founded on the novel reaching

law with PTSM and the novel sliding mode surface with PTSM, is put forward. As far as we are aware, this concept has hitherto remained unexamined.

3.1. Preliminaries

Consider the following nonlinear system equation [39]:

$$\dot{x} = f(t, x; \rho) \tag{11}$$

where $x \in \mathbb{R}^n$ is the system state variable, $\rho \in R^b$ and $\dot{\rho} = 0$ are system parameters, $f : \mathbb{R}^n \to \mathbb{R}^n$ is a function of a nonlinear system, and $t \in [t_0, \infty)$ is time variables, where $t_0 \in [0, \infty)$, $x_0 = x(t_0)$ is the initial value.

Definition 1 ([37,39–41])**.** *Predefined-time synchronization.*

Assuming that the system defined by Equation (11) possesses fixed-time stability, it is feasible to deduce that $f(t, x_0; \rho)$ is capable of converging to the equilibrium point within a prescribed time frame, i.e.,

$$\lim_{t \to T(\rho)} \|x(t)\| \tag{12}$$

where the settling time $T(\rho)$ is solely determined by the parameter ρ, irrespective of the initial value x_0, and is globally bounded. If $x_0 \in \mathbb{R}^n$, there exist $T(\rho) \in [0, \infty)$ and $T(\rho) \leq T_{max}$. Therefore, the system defined by Equation (11) exhibits stability within a predefined time frame, specifically achieving predefined-time synchronization.

Lemma 1 ([31])**.** *The nonlinear system is characterized by non-Lipschitz continuity, given by $\dot{x} = f(x, t)$, with $f(0) = 0$. Assume the existence of a Lyapunov function $V(x)$, along with positive real numbers $A, B, \Gamma > 0$, $0 < \delta < 1$, and $4B\Gamma = A^2$. This Lyapunov function $V(x)$ should be strictly positive for any nonzero x. Then, the following inequality can be satisfied:*

$$\dot{V} \leq -\frac{4}{T_p A (1 - \delta)} \left(AV + B\, V^{\frac{1+\delta}{2}} + \Gamma\, V^{\frac{3-\delta}{2}} \right) \tag{13}$$

Therefore, the system defined as $\dot{x} = f(x)$ exhibits predefined-time stability, with the settling time being determined solely by the predefined-time parameter T_p. Then, the real settling time $T_c(x_0) \leq T_p$.

It is worth noting that the state variables of the closed-loop system can asymptotically converge to the equilibrium point by means of the Lyapunov theorem and LaSalle's invariance principle [42–44].

Lemma 2 ([31])**.** *The PTSM for predefined-time synchronization is presented as follows:*

$$s = \dot{x} + \alpha x + \beta x^{\frac{q}{p}} + \gamma x^{2 - \frac{q}{p}} = 0 \tag{14}$$

where the scalar variable $x(t)$is a real number, the scalar constants $\alpha, \beta, \gamma > 0$, and the positive integers q, p $(q < p)$ are odd.

The system defined as $\dot{x} = f(x)$ can exhibit predefined-time stability, provided that the parameters specified in Equation (14) satisfy the inequalities outlined in Equation (15). In addition, the settling time T_c is determined by the predefined-time parameter T_p, and $T_c(x_0) \leq T_p$.

$$\begin{cases} \alpha \geq \dfrac{4}{T_p\left(1 - \frac{q}{p}\right)} \\ \beta \geq \dfrac{2\mu}{T_p\left(1 - \frac{q}{p}\right)} \\ \gamma \geq \dfrac{2}{T_p \mu \left(1 - \frac{q}{p}\right)} \end{cases} \tag{15}$$

where T_p is predefined-time parameter, and $\mu > 0$.

It is noteworthy to mention that the positive integers q and p in Equation (14) are odd and solely the real solution is taken into account. Consequently, this ensures that the values of the expression x, $\beta x^{q/p}$ and $\gamma x^{2-q/p}$ are consistently real numbers [45].

3.2. Controller Design for Second-Order Nonlinear SISO System

To further discuss practical applications of PTSM, we consider a second-order nonlinear SISO system as follows [46]:

$$\begin{cases} \frac{d}{dt}x_1(t) = x_2(t) \\ \frac{d}{dt}x_2(t) = f(x,t) + r(x,t)u(t) \end{cases} \tag{16}$$

where $x_1(t)$, $x_2(t)$ are system states, with the initial state values $x_1(0)$, $x_2(0)$, $f(x)$ and $r(x)$ are known nonlinear functions, respectively, with smooth vector fields on $\mathbb{R}^1$, $r(x) \neq 0$, and $u(t) \in \mathbb{R}^1$, where $u(t)$ is the control input.

There are usually two steps to design an SMC controller based on Lyapunov stability theory [47]. The initial step involves designing a sliding mode surface, guaranteeing that the system response meets the desired states when the plant operates within the sliding surface. The second step involves creating switched feedback gains that drive the state trajectory towards the sliding surface, which can be optimized by utilizing an appropriate reaching law [46]. Then, the convergence process is divided into two corresponding phases with the settling time $T_c = T_{c0} + T_{c1}$. The first phase is the reaching motion phase, which corresponds to the reaching process in sliding mode control with the settling time T_{c1}. The second phase occurs when the system maintains a sliding mode motion under the control law with the settling time T_{c0}.

3.2.1. The Novel Controller Design with PTSM-LSM

PTSM-LSM refers to the sliding mode design that involves a reaching law with PTSM and a sliding mode surface with linear sliding mode (LSM).

Theorem 1. *A novel reaching law with PTSM is proposed as follows.*

$$\frac{d}{dt}s(t) = -\alpha s(t) - \beta s(t)^{\frac{q}{p}} - \gamma s(t)^{2-\frac{q}{p}} = 0 \tag{17}$$

where α, β, $\gamma > 0$, q, p are positive odd integers, and $q < p$.

The novel reaching law $s(t)$ can have predefined-time stability on the condition that the parameters of Equation (17) meet the inequalities in Equation (15). In addition, the settling time $T_c(s_0)$ required to transition from any initial state $s(t_0) \neq 0$ to the equilibrium state $s(t_c) = 0$ on the sliding mode is determined by the predefined-time parameter T_p, and $T_c(s_0) \leq T_p$.

Equation (17) can be rewritten as Equation (14). The proof for the predefined-time stability of Equation (17) follows a similar approach to that outlined in Lemma 2. Therefore, it will not be reiterated here.

It is worth noting that the novel reaching law with PTSM (Equation (17)) has predefined-time stability, which will provide convenience for designing the parameters to adjust the reaching speed of the variable index reaching law. In addition, the introduction of the system state variable with no sign functions and the power order term of the sliding mode function effectively mitigates the shortcomings associated with the chattering phenomenon.

Theorem 2. *A novel approach to designing the controller (Equation (20)) for second-order nonlinear SISO systems (Equation (16)) involves the application of PTSM-LSM.*

$$u(t) = -\frac{1}{r(x,t)}\left(f(x,t) + c\,x_2 + \alpha_1\,s_1 + \beta_1\,s_1^{\frac{q_1}{p_1}} + \gamma_1\,s_1^{2-\frac{q_1}{p_1}} \right) \tag{18}$$

where $\alpha_1, \beta_1, \gamma_1 > 0, q_1, p_1$ are positive odd integers, and $q_1 < p_1$.

The systems in Equation (16) can have predefined-time stability on the condition that the parameters of Equation (18) meet the following inequalities in Equation (19). In addition, the settling time T_{c1} for the reaching motion phase is determined by the predefined-time parameter T_{p1}, and $T_{c1} \leq T_{p1}$. The settling time T_{c0} for the sliding mode motion phase is determined by the parameter c. Then, the total settling time T_c for the system (Equation (10)) is determined by the predefined-time parameter T_{p1} and T_{c0}, i.e., $T_c(x_0) \leq T_{c0} + T_{p1}$, where $T_c = T_{c0} + T_{c1}$.

$$\begin{cases} \alpha_1 \geq \dfrac{4}{T_{p1}\left(1-\frac{q_1}{p_1}\right)} \\[2mm] \beta_1 \geq \dfrac{2\mu_1}{T_{p1}\left(1-\frac{q_1}{p_1}\right)} \\[2mm] \gamma_1 \geq \dfrac{2}{T_{p1}\,\mu_1\left(1-\frac{q_1}{p_1}\right)} \end{cases} \tag{19}$$

where $\mu_1 = \sqrt{\beta_1}\,/\,\sqrt{\gamma_1}, \mu_1 > 0$, T_{p1} is the predefined-time parameter.

Proof of Theorem 2.

Step 1. Sliding mode surface

Based on the Lyapunov stability theory, a sliding mode surface with LSM is designed as follows.

$$s_1(t) = \dot{x}_1(t) + cx_1(t) \tag{20}$$

where c satisfies the Hurwitz condition, i.e., $c > 0$.

Suppose the settling time T_{c0}, which refers to the phase of sliding mode motion under the control law, is determined by the parameter c.

Step 2. Reaching law

The reaching law with PTSM is designed as follows according to Theorem 1.

$$\frac{d}{dt}s_1(t) = -\alpha_1\,s_1 - \beta_1\,s_1^{\frac{q_1}{p_1}} - \gamma_1\,s_1^{2-\frac{q_1}{p_1}} \tag{21}$$

where $\alpha_1, \beta_1, \gamma_1 > 0, q_1, p_1$ are positive odd integers, and $q_1 < p_1$. The parameters specified in Equation (20) adhere to the conditions outlined in Equation (19).

Then, the settling time T_{c1} for the reaching motion phase is determined by the predefined-time parameter T_{p1}, and $T_{c1} \leq T_{p1}$.

Step 3. Stability analysis

The Lyapunov function is designed as follows.

$$V(t) = \frac{1}{2}s_1(t)^2 \tag{22}$$

Then, the derivative of $V(t)$ is derived by combining Equations (16), (18), and (20).

$$\begin{aligned} \frac{d}{dt}V(t) &= s_1(t)\big(\dot{x}_2(t) + cx_2(t)\big) \\ &= s_1(t)\big(f(x,t) + r(x,t)u(t) + cx_2(t)\big) \\ &= s_1(t)\left(-\alpha_1\,s_1 - \beta_1\,s_1^{\frac{q_1}{p_1}} - \gamma_1\,s_1^{2-\frac{q_1}{p_1}} \right) \\ &= -\alpha_1\,s_1(t)^2 - \beta_1 s_1(t)^{\frac{p_1+q_1}{p_1}} - \gamma_1\,s_1(t)^{\frac{3p_1-q_1}{p_1}} \end{aligned} \tag{23}$$

Since both $(p_1 + q_1)$ and $(3p_1 - q_1)$ are positive even numbers, it can be inferred that the inequalities $s_1(t)^{(p_1+q_1)/p_1} > 0$ and $s_1(t)^{(3p_1-q_1)/p_1} > 0$ in Equation (23) are valid, i.e., $\dot{V}(t) \leq 0$. Then, the stability of the second-order nonlinear SISO system (Equation (16)) has been proved. □

3.2.2. The Novel Controller Design with PTSM-PTSM

PTSM-PTSM refers to the sliding mode design that involves a reaching law with PTSM and a sliding mode surface with PTSM.

Theorem 3. *A novel sliding mode surface with PTSM is proposed as follows.*

$$s(t) = x_2 + \alpha_0 x_1 + \beta_0 x_1^{\frac{q_0}{p_0}} + \gamma_0 x_1^{2-\frac{q_0}{p_0}} \tag{24}$$

where $\alpha_0, \beta_0, \gamma_0 > 0$, q_0, p_0 are positive odd integers, and $q_0 < p_0$.

The novel sliding mode surface $s(t)$ can have predefined-time stability on the condition that the parameters of Equation (24) meet the inequalities in Equation (15). In addition, the settling time $T_{c0}(s(t_0))$ from any initial state $s(t_0) \neq 0$ to the equilibrium state $s(t_c) = 0$ on the sliding mode is determined by the predefined-time parameter T_{p0}, and $T_{c0}(s(t_1)) \leq T_{p0}$.

Equation (24) can be rewritten as Equation (14). The proof for the predefined-time stability of Equation (24) follows a similar approach to that outlined in Lemma 2. Therefore, it will not be reiterated here.

It is worth noting that the novel sliding mode surface with PTSM (Equation (24)) has predefined-time stability, which will provide convenience for designing the parameters to adjust the sliding mode motion of the variable index sliding mode surface.

Theorem 4. *A novel approach to designing the SPTSM controller for second-order nonlinear SISO systems (Equation (16)) involves the application of PTSM-PTSM, as in Equation (25).*

$$u(t) = -\frac{1}{r(x,t)}\left(f(x,t) + \alpha_0 x_2 + \frac{\beta_0 q_0 x_2 x_1^{\frac{q_0}{p_0}-1}}{p_0} + \gamma_0\left(2 - \frac{q_0}{p_0}\right) x_2 x_1^{1-\frac{q_0}{p_0}} + \alpha_1 s_1 + \beta_1 s_1^{\frac{q_1}{p_1}} + \gamma_1 s_1^{2-\frac{q_1}{p_1}} \right) \tag{25}$$

where $\alpha_i, \beta_i, \gamma_i > 0$, q_i, p_i are positive odd integers, and $q_i < p_i$, with $i = 0, 1$.

The system in Equation (16) can have predefined-time stability on the condition that the parameters of Equation (25) meet the following inequalities in Equation (26). In addition, the settling time T_{c1} for the reaching motion phase is determined by the predefined-time parameter T_{p1}, and $T_{c1} \leq T_{p1}$. The settling time T_{c0} for the sliding mode motion phase is determined by the predefined-time parameter T_{p0}, and $T_{c0} \leq T_{p0}$. Then, the total settling time T_c for the system (Equation (10)) is determined by the predefined-time parameter T_p, and $T_c(x_0) \leq T_p$, where $T_c = T_{c0} + T_{c1}$, $T_p = T_{p0} + T_{p1}$.

$$\begin{cases} \alpha_i \geq \dfrac{4}{T_{pi}\left(1-\frac{q_i}{p_i}\right)} \\ \beta_i \geq \dfrac{2\mu_i}{T_{pi}\left(1-\frac{q_i}{p_i}\right)} \\ \gamma_i \geq \dfrac{2}{T_{pi}\mu_i\left(1-\frac{q_i}{p_i}\right)} \end{cases} \tag{26}$$

where $\mu_i = \sqrt{\beta_i}/\sqrt{\gamma_i}$, $\mu_i > 0$, T_{pi} is the predefined-time parameter, with $i = 0, 1$.

Proof of Theorem 4.

Step 1. Sliding mode surface

Based on Lyapunov stability theory, a sliding mode surface with PTSM is designed the same as Equation (24) according to Theorem 3.

Suppose the settling time T_{c0}, which refers to the phase of sliding mode motion under the control law, is determined by the predefined-time parameter T_{p0}, and $T_{c0} \le T_{p0}$.

Then, the derivative of Equation (24) is derived as follows.

$$\frac{d}{dt}s(t) = \dot{x}_2 + \alpha_0\,x_2 + \frac{\beta_0\,q_0\,x_2\,x_1^{\frac{q_0}{p_0}-1}}{p_0} + \gamma_0\left(2 - \frac{q_0}{p_0}\right)x_2\,x_1^{1-\frac{q_0}{p_0}} \tag{27}$$

Step 2. Reaching law

The reaching law with PTSM is designed the same as Equation (21) according to Theorem 1.

Then, the settling time T_{c1} for the reaching motion phase is determined by the predefined-time parameter T_{p1}, and $T_{c1} \le T_{p1}$.

Then, the total settling time T_c for the system (Equation (10)) is determined by the predefined-time parameter T_p, and $T_c(x_0) \le T_p$, where $T_c = T_{c0} + T_{c1}$, $T_p = T_{p0} + T_{p1}$.

Step 3. Stability analysis

The Lyapunov function is designed as follows.

$$V(t) = \frac{1}{2}s_1(t)^2 \tag{28}$$

Then, the derivative of $V(t)$ is derived by combining Equation (16), (18), and (25).

$$\begin{aligned}
\frac{d}{dt}V(t) &= s_1(t)\left(\dot{x}_2(t) + \alpha_0\,x_2 + \frac{\beta_0\,q_0\,x_2\,x_1^{\frac{q_0}{p_0}-1}}{p_0} + \gamma_0\left(2 - \frac{q_0}{p_0}\right)x_2\,x_1^{1-\frac{q_0}{p_0}}\right) \\
&= s_1(t)\left(f(x,t) + r(x,t)u(t) + \alpha_0\,x_2 + \frac{\beta_0\,q_0\,x_2\,x_1^{\frac{q_0}{p_0}-1}}{p_0} + \gamma_0\left(2 - \frac{q_0}{p_0}\right)x_2\,x_1^{1-\frac{q_0}{p_0}}\right) \\
&= s_1(t)\left(-\alpha_1\,s_1 - \beta_1\,s_1^{\frac{q_1}{p_1}} - \gamma_1\,s_1^{2-\frac{q_1}{p_1}}\right) \\
&= -\alpha_1\,s_1(t)^2 - \beta_1 s_1(t)^{\frac{p_1+q_1}{p_1}} - \gamma_1\,s_1(t)^{\frac{3p_1-q_1}{p_1}}
\end{aligned} \tag{29}$$

Since both $(p_1 + q_1)$ and $(3p_1 - q_1)$ are positive even numbers, it can be inferred that the inequalities $s_1(t)^{(p_1+q_1)/p_1} > 0$ and $s_1(t)^{(3p_1-q_1)/p_1} > 0$ in Equation (29) are valid, i.e., $\dot{V}(t) \le 0$. Then, the stability of the second-order nonlinear SISO system (Equation (16)) has been proved. □

3.2.3. The Robust Controller Design with PTSM-PTSM

To further explore the practical application scope of *the SPTSM controller (Equation (25))*, we consider an uncertain second-order nonlinear SISO system, as in Equation (30).

$$\begin{cases} \frac{d}{dt}x_1 = x_2 \\ \frac{d}{dt}x_2 = f(x,t) + r(x,t)u(t) + d(x,t) \end{cases} \tag{30}$$

where $d(x,t)$ is the total uncertainty, which includes system parameter uncertainties and external disturbances. It is assumed that this total uncertainty has an upper bound D, i.e., $|d(x,t)| \le D$. $x_1(t)$, $x_2(t)$ are system states, with the initial state values $x_1(0)$, $x_2(0)$. $f(x)$ and $r(x)$ are known nonlinear functions, respectively, with smooth vector fields on $\mathbb{R}^1$, $r(x) \ne 0$, and $u(t) \in \mathbb{R}^1$, where $u(t)$ is the control input.

Based on Theorem 4, this paper presents a new approach to SPTSM for an uncertain second-order nonlinear SISO system as Theorem 5.

Theorem 5. *A novel approach to designing the robust SPTSM controller for uncertain second-order nonlinear SISO systems (Equation (30)) involves the application of PTSM-PTSM, as in Equation (31).*

$$u(t) = -\frac{1}{r(\boldsymbol{x},t)}\left(f(\boldsymbol{x},t) + \alpha_0\, x_2 + \frac{\beta_0\, q_0\, x_2\, x_1^{\frac{q_0}{p_0}-1}}{p_0} + \gamma_0\left(2 - \frac{q_0}{p_0}\right)x_2\, x_1^{1-\frac{q_0}{p_0}} + \alpha_1\, s_1 + \beta_1\, s_1^{\frac{q_1}{p_1}} + \gamma_1\, s_1^{2-\frac{q_1}{p_1}} \right) \tag{31}$$

where $\alpha_1 > D/|s_1|$, $\alpha_i, \beta_i, \gamma_i > 0$, q_i, p_i are positive odd integers, and $q_i < p_i$, with $i = 0, 1$.

The system in Equation (30) can have predefined-time stability on the condition that the parameters of Equation (31) meet the following inequalities in Equation (32). In addition, the settling time T_{c1} for the reaching motion phase is determined by the predefined-time parameter T_{p1}, and $T_{c1} \leq T_{p1}$. The settling time T_{c0} for the sliding mode motion phase is determined by the predefined-time parameter T_{p0}, and $T_{c0} \leq T_{p0}$. Then, the total settling time T_c for the system (Equation (30)) is determined by the predefined-time parameter T_p, and $T_c(x_0) \leq T_p$, where $T_c = T_{c0} + T_{c1}$, $T_p = T_{p0} + T_{p1}$.

$$\begin{cases} \alpha_i \geq \dfrac{4}{T_{pi}\left(1-\frac{q_i}{p_i}\right)} \\[2mm] \beta_i \geq \dfrac{2\mu_i}{T_{pi}\left(1-\frac{q_i}{p_i}\right)} \\[2mm] \gamma_i \geq \dfrac{2}{T_{pi}\mu_i\left(1-\frac{q_i}{p_i}\right)} \end{cases} \tag{32}$$

where $\mu_i = \sqrt{\beta_i}/\sqrt{\gamma_i}$, $\mu_i > 0$, T_{pi} is the predefined-time parameter, with $i = 0, 1$.

Proof of Theorem 5 .

Step 1. Stability and convergence analysis

The Lyapunov function is designed as Equation (33).

$$V(t) = \frac{1}{2}s_1{}^2 \tag{33}$$

Combine Equations (16), (24), and (25). Then, the derivative of $V(t)$ can be derived as follows.

$$\begin{aligned} \dot{V}(t) &= s_1 \dot{s}_1 \\ &= s_1\left(\dot{x}_2 + \alpha_0\, x_2 + \frac{\beta_0\, q_0}{p_0} x_2\, x_1^{\frac{q_0}{p_0}-1} + \gamma_0\left(2 - \frac{q_0}{p_0}\right)x_2\, x_1^{1-\frac{q_0}{p_0}} \right) \\ &= s_1\left(\begin{array}{l} f(\boldsymbol{x},t) + r(\boldsymbol{x},t)u(t) + d(\boldsymbol{x},t) + \alpha_0\, x_2 + \frac{\beta_0\, q_0}{p_0} x_2\, x_1^{\frac{q_0}{p_0}-1} \\ + \gamma_0\left(2 - \frac{q_0}{p_0}\right)x_2\, x_1^{1-\frac{q_0}{p_0}} \end{array} \right) \\ &= s_1\left(-\alpha_1\, s_1 - \beta_1\, s_1^{\frac{q_1}{p_1}} - \gamma_1\, s_1^{2-\frac{q_1}{p_1}} + d(\boldsymbol{x},t) \right) \\ &= -\left(\alpha_1 - \frac{d(\boldsymbol{x},t)}{s_1} \right) s_1{}^2 - \beta_1 s_1^{\frac{p_1+q_1}{p_1}} - \gamma_1 s_1^{\frac{3p_1-q_1}{p_1}} \\ &= -\alpha_1' s_1{}^2 - \beta_1 s_1^{\frac{p_1+q_1}{p_1}} - \gamma_1 s_1^{\frac{3p_1-q_1}{p_1}} \end{aligned} \tag{34}$$

where $\alpha_1' = \alpha_1 - d(\boldsymbol{x},t)/s_1$.

It follows that the existence of $|d(\boldsymbol{x},t)| \leq D$ and $\alpha_1 > D/|s_1|$ is equivalent to the existence of $\alpha_1' > 0$. Since both $(p_1 + q_1)$ and $(3p_1 - q_1)$ are positive even numbers, the two power terms in Equation (34) satisfy $s_1^{(p_1+q_1)/p_1} > 0$ and $s_1^{(3p_1-q_1)/p_1} > 0$, such

that $\dot{V}(t) \leq 0$ holds. Since the stability and convergence analysis is achieved, the uncertain system (Equation (30)), with the robust SPTSM controller (Equation (31)), has Lyapunov stability.

On further analysis, however, it was noticed that there is the existence of $\alpha_1 > D/|s_1|$, i.e., $|s_1| > D/\alpha_1$; then, the system state reaches the neighborhood Δ of the sliding mode surface $s_1 = 0$.

$$\Delta = \left\{ x : |s_1| \leq \frac{D}{\alpha_1} \right\} \tag{35}$$

This is such that if there exists a sufficiently large value of scalar α_1, the neighborhood Δ of the sliding mode surface $s_1 = 0$ can be made small enough.

Step 2. Predefined-time stability analysis

The expression of Equation (34) can be written as follows:

$$\dot{V}(t) = -\left(\alpha_1' V + \beta_1 V^{\frac{1+\delta}{2}} + \gamma_1 V^{\frac{3-\delta}{2}} \right) \tag{36}$$

where $\delta = q/p, 0 < \delta < 1$.

Comparing to the parameter condition Equation (15) for Lemma 2, the system parameter condition Equation (37) for the Lyapunov function Equation (36) is derived.

$$\begin{cases} \alpha_1' \geq \frac{4}{T_p(1-\delta)} \\ \beta_1 \geq \frac{2\sqrt{B}}{T_p\sqrt{\Gamma}(1-\delta)} \\ \gamma_1 \geq \frac{2\sqrt{\Gamma}}{T_p\sqrt{B}(1-\delta)} \end{cases} \tag{37}$$

It follows that the condition in Equation (37) is equivalent to the condition in Equation (15), with $\mu = \sqrt{B}/\sqrt{\Gamma}$, $\mu > 0$. The detailed proof process will not be elaborated here.

Then, the predefined-time stability analysis is achieved and the condition Equation (32) is derived. □

3.3. SPTSM Controller Design for Speed Regulation System of PMSM

In this section, we design the SPTSM controller for the second-order state equation of the speed regulation system of a PMSM (Equation (10)) with PTSM-PTSM.

Based on Theorem 5, the following robust controller (Equation (38)) for the speed regulation system (Equation (10)) is designed with SPTSM.

$$i_{qref} = \frac{2J}{3P_n\psi_f} \int_0^t \left(\frac{1}{J} B\dot{\omega}_m + \alpha_0 x_2 + \frac{\beta_0 q_0 x_2 x_1^{\frac{q_0}{p_0}-1}}{p_0} + \gamma_0 \left(2 - \frac{q_0}{p_0} \right) x_2 x_1^{1-\frac{q_0}{p_0}} + \alpha_1 s_1 + \beta_1 s_1^{\frac{q_1}{p_1}} + \gamma_1 s_1^{2-\frac{q_1}{p_1}} \right) d\tau \tag{38}$$

where $\alpha_1 > D/|s_1|$, $\alpha_i, \beta_i, \gamma_i > 0$, q_i, p_i are positive odd integers, and $q_i < p_i$, with $i = 0, 1$.

The systems in Equation (10) can have predefined-time stability on the condition that the parameters specified in the robust controller (Equation (38)) adhere to the set of inequalities as stated in Equation (32). In addition, the settling time T_{c1} for the reaching motion phase is determined by the predefined-time parameter T_{p1}, and $T_{c1} \leq T_{p1}$. The settling time T_{c0} for the sliding mode motion phase is determined by the predefined-time parameter T_{p0}, and $T_{c0} \leq T_{p0}$. Then, the total settling time T_c for the system (Equation (10)) is determined by the predefined-time parameter T_p, and $T_c(x_0) \leq T_p$, where $T_c = T_{c0} + T_{c1}$, $T_p = T_{p0} + T_{p1}$.

Equation (38) is equivalent to Equation (31). The proof for the predefined-time stability of controller Equation (38) follows a similar approach to that outlined in Theorem 5. Therefore, it will not be reiterated here.

A block diagram of the SPTSM controller (Equation (38)) design with PTSM-PTSM is presented in Figure 1.

Figure 1. Block diagram of the SPTSM controller design with PTSM-PTSM.

4. Results and Discussion

The novel controllers for the second-order state equation of the speed regulation system of a PMSM (Equation (10)) can be used to control the speed loop current i_{qref}, provided that the rest of the system has been fully verified. In the following sections, the simulation and experiment results of the controller for the second-order state equation of the speed regulation system of a PMSM (Equation (10)) will verify the effectiveness of PTSM. The control block diagram of the PMSM control system is shown in Figure 2.

Figure 2. Control block diagram of the PMSM control system.

4.1. Parameters of PMSM

The parameters of the PMSM used for simulation and experiment validation are shown in Table 1.

Table 1. System parameters of the PMSM.

Name	Symbol	Value and Unit
Maximum power	P_{max}	400 W
DC-link voltage	U_{DC}	48 V
Number of pole pairs	P_n	4
Resistance (ph-ph)	R	$0.15 \pm 10\%~\Omega$

Table 1. *Cont.*

Name	Symbol	Value and Unit
Inductance (ph-ph)	L	$0.708 \pm 10\%$ mH
Permanent-magnet flux linkage	ψ_f	1.56×10^{-2} Wb
Inertia	J	2.9×10^{-4} kg·m^2
Maximum speed.	N_{max}	3×10^3 r/min

4.2. Influence of Controller Parameters

Based on Theorem 5, the SPTSM controller (Equation (38)), which exhibits predefined-time stability, is subject to seven crucial factors, T_{p0}, μ_0, q_0/p_0, T_{p1}, μ_1, q_1/p_1, and initial states. The variable under investigation is the sole factor specified in each group of experiments for comparison. Then, we design the parameters identically, with the exception of a sole factor specified for each group, and establish an identical initial value to guarantee fairness. The comparative simulation experiments for each factor are individually applied to three groups.

It is worth noting that PTSM-PTSM, which makes some improvements in the design of the sliding surface based on PTSM-LSM, has a better control effect in theory. Therefore, we focus on PTSM-PTSM in this section. In addition, the main content of this section focuses on several factors that have a significant impact on the effects of system convergence, and other factors are not discussed here.

4.2.1. Comparison Results of Different T_{p0}

The parameters that are specified in the robust controller (Equation (38)) adhere to the set of inequalities as stated in Equation (32), which are, respectively, designed the same in the three comparative groups as $\mu_0 = 0.5$, $q_0/p_0 = 3/5$, $T_{p1} = 0.1$, $\mu_1 = 0.1$, and $q_1/p_1 = 3/5$. For the variable under investigation, the value of the parameter of predefined-time T_{p0} is assigned as $T_{p0(a)} = 0.3$, $T_{p0(b)} = 0.6$, and $T_{p0(c)} = 0.9$, *respectively*, in each comparative group.

The value of parameters that are not considered as subjects of this study in the controller (Equation (38)) for simulations are calculated by considering the inequalities with an equal sign in Equation (32), as presented in Table 2.

Table 2. The parameters of the controller (Equation (38)) with different T_{p0}.

Group	α_0	β_0	γ_0	q_0/p_0	α_1	β_1	γ_1	q_1/p_1
(a)	33.33	8.33	33.33	0.6	100	5	500	0.6
(b)	16.67	4.17	16.67	0.6	100	5	500	0.6
(c)	11.11	2.78	11.11	0.6	100	5	500	0.6

The reference speed N_{ref} is set to 1000 r/min in the simulations. The PMSM starts with only the inherent load T_{Lin} and the inherent viscous frictional coefficient B_{in} of the system. Then, the load increases suddenly to 1 N·m at 0.3 s.

The comparison curves of different T_{p0} are presented in Figure 3. At first, the relationship among the total convergence times is $T_{c(a)} < \left(T_{p0(a)} + T_{p1(a)}\right)$, $T_{c(b)} < \left(T_{p0(b)} + T_{p1(b)}\right)$, $T_{c(c)} < \left(T_{p0(c)} + T_{p1(c)}\right)$, which verifies the conclusion that the total settling time T_c for the system is determined by the predefined-time parameter T_p, and $T_c(x_0) \leq T_p$, where $T_c = T_{c0} + T_{c1}$, $T_p = T_{p0} + T_{p1}$. Then, the total settling time $T_{c(a)} < T_{c(b)} < T_{c(c)}$ indicates that as the predefined-time parameter T_{p0} of the novel sliding surface with PTSM increases, the total settling time T_c of the control system increases.
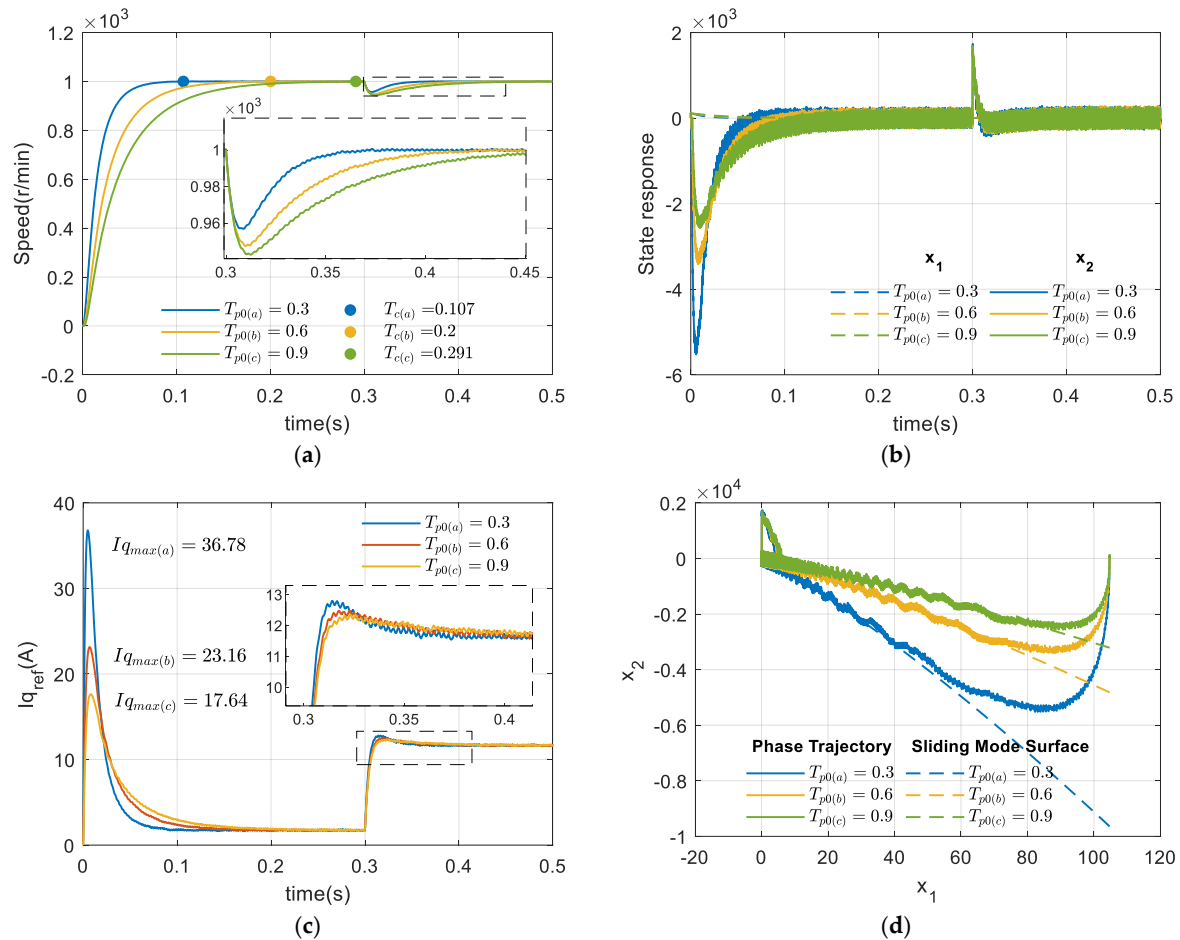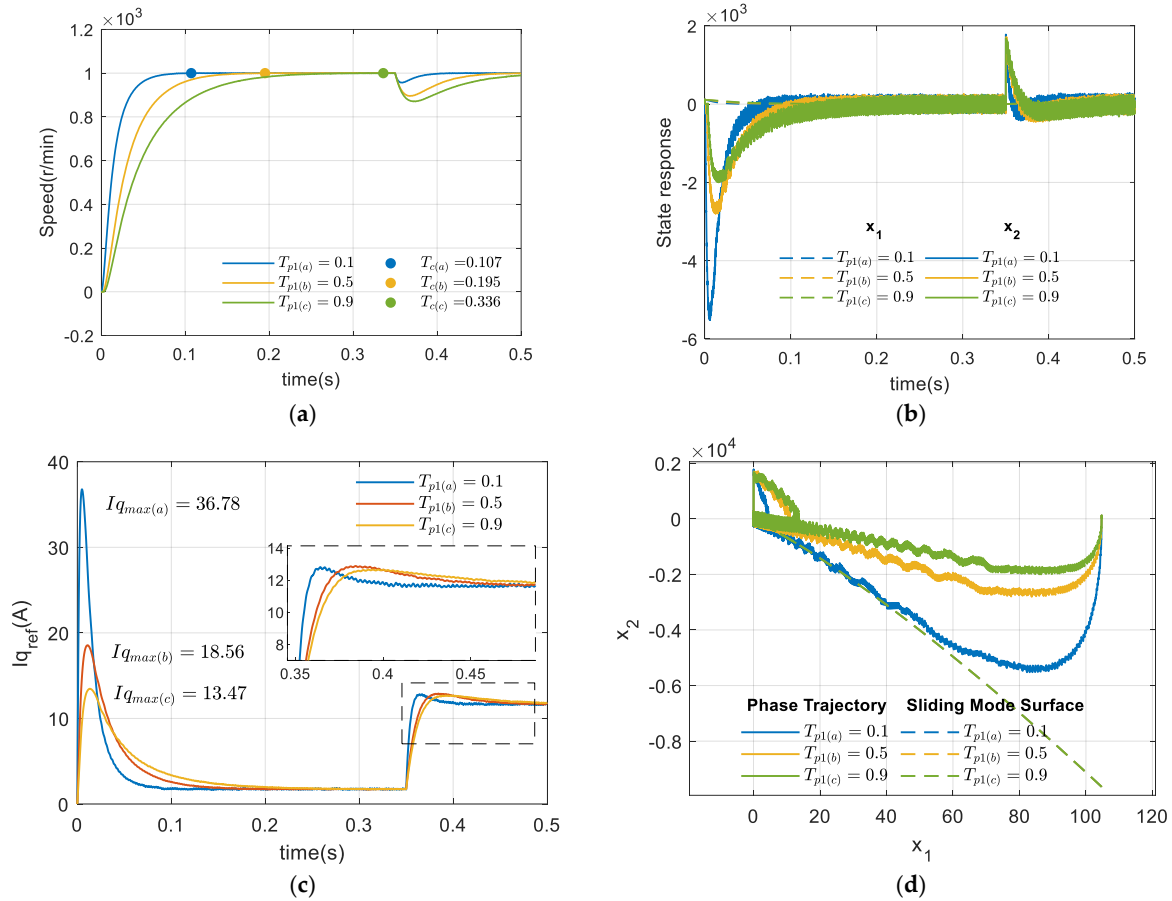
Figure 3. Comparison results of different T_{p0}. (**a**) Speed tracking, (**b**) state responses, (**c**) control inputs, and (**d**) phase trajectories.

4.2.2. Comparison Results of Different T_{p1}

The parameters that are specified in the robust controller (Equation (38)) adhere to the set of inequalities as stated in Equation (32), which are, respectively, designed the same in the three comparative groups as $T_{p0} = 0.3$, $\mu_0 = 0.5$, $q_0/p_0 = 3/5$, $\mu_1 = 0.1$, and $q_1/p_1 = 3/5$. For the variable under investigation, the value of the parameter of predefined-time T_{p1} is assigned as $T_{p1(a)} = 0.1$, $T_{p1(b)} = 0.5$, and $T_{p1(c)} = 0.9$, *respectively*, in each comparative group.

The value of parameters that are not considered as subjects of this study in the controller (Equation (38)) for simulations are calculated by considering the inequalities with an equal sign in Equation (32), as presented in Table 3.

The reference speed N_{ref} is set to 1000 r/min in the simulations. The PMSM starts with only the inherent load T_{Lin} and the inherent viscous frictional coefficient B_{in} of the system. Then, the load increases suddenly to 1 N·m at 0.35 s.

Table 3. The parameters of the controller (Equation (38)) with different T_{p1}.

Group	α_0	β_0	γ_0	q_0/p_0	α_1	β_1	γ_1	q_1/p_1
(a)	33.33	8.33	33.33	0.6	100	5	500	0.6
(b)	33.33	8.33	33.33	0.6	20	1	100	0.6
(c)	33.33	8.33	33.33	0.6	11.11	0.56	55.56	0.6

The comparison curves of different T_{p1} are presented in Figure 4. At first, the relationship among the total convergence times is $T_{c(a)} < \left(T_{p0(a)} + T_{p1(a)} \right)$, $T_{c(b)} < \left(T_{p0(b)} + T_{p1(b)} \right)$, $T_{c(c)} < \left(T_{p0(c)} + T_{p1(c)} \right)$, which verifies the conclusion that the total settling time T_c for the system is determined by the predefined-time parameter T_p, and $T_c(x_0) \leq T_p$, where $T_c = T_{c0} + T_{c1}$, $T_p = T_{p0} + T_{p1}$. Then, the total settling time $T_{c(a)} < T_{c(b)} < T_{c(c)}$ indicates that as the predefined-time parameter T_{p1} of the novel reaching law with PTSM increases, the total settling time T_c of the control system increases.

Figure 4. Comparison results of different T_{p1}. (**a**) Speed tracking, (**b**) state responses, (**c**) control inputs, and (**d**) phase trajectories.

4.2.3. Comparison Results of Different μ_0

The parameters that are specified in the robust controller (Equation (38)) adhere to the set of inequalities as stated in Equation (32), which are, respectively, designed the same in the three comparative groups as $T_{p0} = 0.3$, $q_0/p_0 = 3/5$, $T_{p1} = 0.1$, $\mu_1 = 0.1$, and $q_1/p_1 = 3/5$. For the variable under investigation, the value of parameter μ_0 is assigned as $\mu_{0(a)} = 0.3$, $\mu_{0(b)} = 1.0$, and $\mu_{0(c)} = 1.5$, *respectively*, in each comparative group.

The value of parameters that are not considered as subjects of this study in the controller (Equation (38)) for simulations are calculated by considering the inequalities with an equal sign in Equation (32), as presented in Table 4.

The reference speed N_{ref} is set to 1000 r/min in the simulations. The PMSM starts with only the inherent load T_{Lin} and the inherent viscous frictional coefficient B_{in} of the system. Then, the load increases suddenly to 1 N·m at 0.15s.

Table 4. The parameters of the controller (Equation (38)) with different μ_0.

Group	α_0	β_0	γ_0	q_0/p_0	α_1	β_1	γ_1	q_1/p_1
(a)	33.33	5.00	55.56	0.6	100	5	500	0.6
(b)	33.33	16.67	16.67	0.6	100	5	500	0.6
(c)	33.33	25.00	11.11	0.6	100	5	500	0.6

From the comparison curves of different μ_0 presented in Figure 5, the relationship among the total convergence times is $T_{c(a)} \approx T_{c(b)} \approx T_{c(c)}$, which indicates that the parameter μ_0 of the novel sliding surface with PTSM does not affect total settling time T_c of the system, but it will change the convergence rate and phase trajectories. Then, the control output i_{qref} becomes more gradual when the value of μ_0 decreases, which is beneficial for the control system.
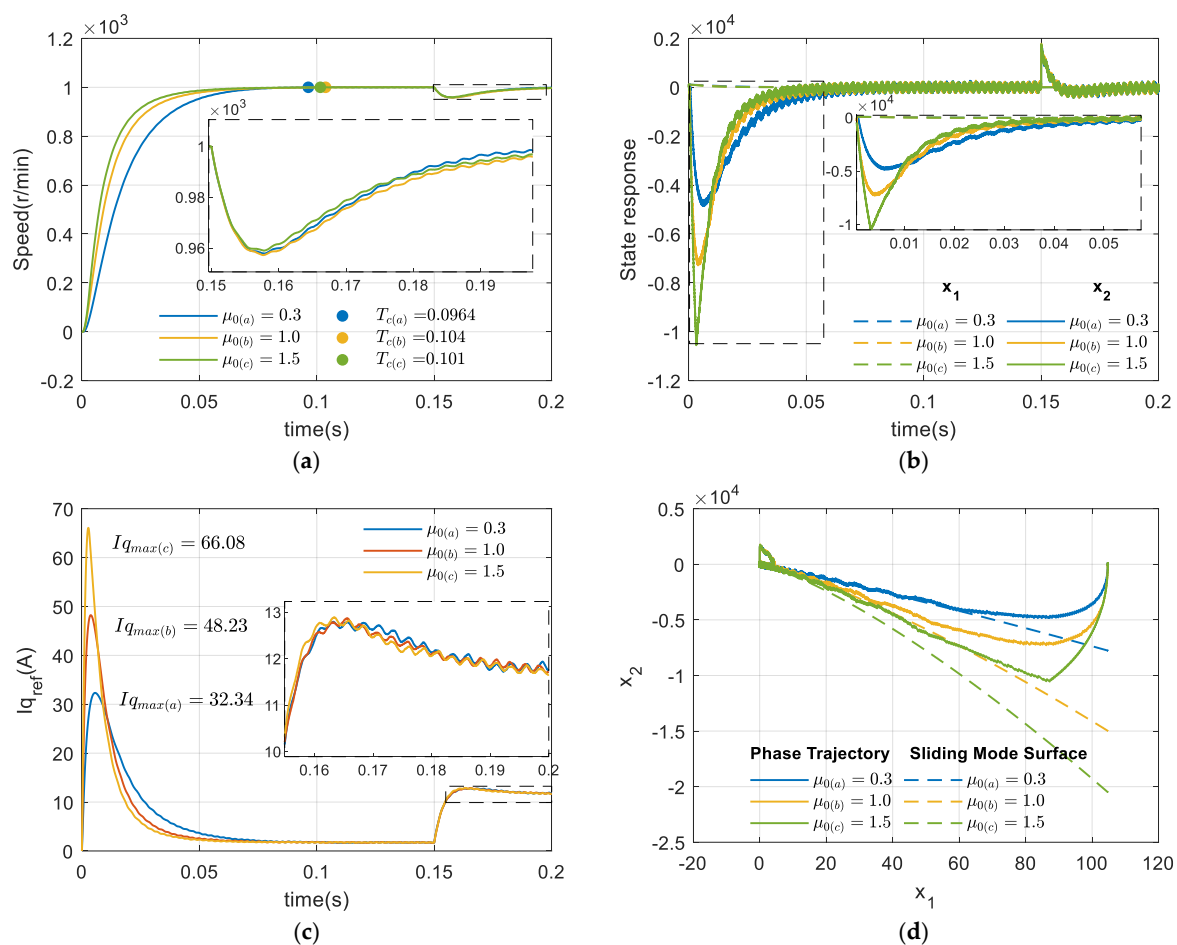
Figure 5. Comparison results of different μ_0. (**a**) Speed tracking, (**b**) state responses, (**c**) control inputs, and (**d**) phase trajectories.

4.2.4. Comparison Results of Different δ_0

The parameters that are specified in the robust controller (Equation (38)) adhere to the set of inequalities as stated in Equation (32), which are, respectively, designed the same in the three comparative groups as $T_{p0} = 0.3$, $\mu_0 = 0.5$, $T_{p1} = 0.1$, $\mu_1 = 0.1$, and $q_1/p_1 = 3/5$. For the variable under investigation, the value of parameter q_0/p_0 is assigned as $\delta_{0(a)} = 3/5$, $\delta_{0(b)} = 5/7$, and $\delta_{0(c)} = 7/9$, respectively, in each comparative group.

The value of parameters that are not considered as subjects of this study in the controller (Equation (38)) for simulations are calculated by considering the inequalities with an equal sign in Equation (32), as presented in Table 5.

Table 5. The parameters of the controller (Equation (38)) with different δ_0, where $\delta_0 = q_0/p_0$.

Group	α_0	β_0	γ_0	q_0/p_0	α_1	β_1	γ_1	q_1/p_1
(a)	33.33	8.33	33.33	0.600	100	5	500	0.6
(b)	46.67	11.67	46.67	0.714	100	5	500	0.6
(c)	60.00	15.00	60.00	0.778	100	5	500	0.6

The reference speed N_{ref} is set to 1000 r/min in the simulations. The PMSM starts with only the inherent load T_{Lin} and the inherent viscous frictional coefficient B_{in} of the system. Then, the load increases suddenly to 1 N·m at 0.35 s.

From the comparison curves of different δ_0 presented in Figure 6, the relationship among the total convergence times is $T_{c(a)} > T_{c(b)} > T_{c(c)}$, which indicates that the smaller the value of the parameter δ_0 of the novel sliding surface with PTSM is, the longer it takes to reach convergence.
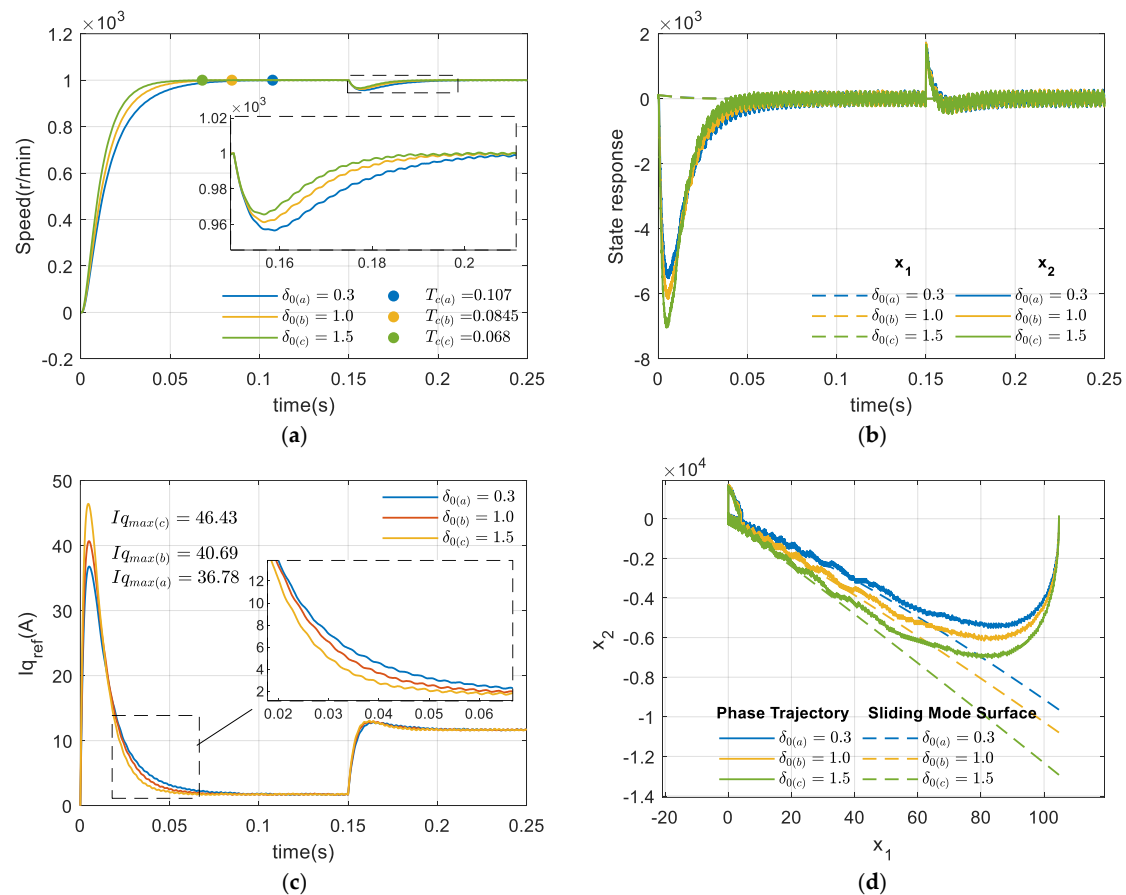
Figure 6. Comparison results of different δ_0. (**a**) Speed tracking, (**b**) state responses, (**c**) control inputs, and (**d**) phase trajectories.

4.3. Comparative Simulation

4.3.1. Comparative Controllers Design

For comparison, we introduce the FTSM to design the controllers for the second-order state equation of the speed regulation system of a PMSM (Equation (10)) with FTSM-LSM and FTSM-FMSM. The FTSM-LSM refers to the sliding mode design that involves a

reaching law with FTSM and a sliding mode surface with linear sliding mode (LSM). The FTSM-FTSM, which makes some improvements in the design of the sliding surface based on FTSM-LSM, refers to the sliding mode design that involves a reaching law with FTSM and a sliding mode surface with FTSM.

1. Controller design with PTSM-LSM

Based on Theorem 2, the following controller (Equation (39)) for the system in Equation (10) is designed with PTSM-LSM.

$$i_{qref} = \frac{2J}{3P_n\psi_f} \int_0^t \left(\frac{1}{J}B\dot{\omega}_m + c\,x_2 + \alpha_1\,s_1 + \beta_1\,s_1^{\frac{q_1}{p_1}} + \gamma_1\,s_1^{2-\frac{q_1}{p_1}} \right) d\tau \tag{39}$$

where $\alpha_1,\ \beta_1,\ \gamma_1 > 0$, q_1, p_1 are positive odd integers, and $q_1 < p_1$.

Equation (39) is equivalent to Equation (18). The proof for the predefined-time stability of the controller in Equation (39) follows a similar approach to that outlined in Theorem 2. Therefore, it will not be reiterated here.

2. Controller design with FTSM-LSM

The following controller Equation (40) for the system in Equation (10) is designed with FTSM-LSM.

$$i_{qref} = \frac{2J}{3P_n\psi_f} \int_0^t \left(\frac{1}{J}B\dot{\omega}_m + c\,x_2 + \alpha_1\,s_1 + \beta_1\,s_1^{\frac{q_1}{p_1}} \right) d\tau \tag{40}$$

where $\alpha_1, \beta_1, \gamma_1 > 0$, q_1, p_1 are positive odd integers, and $q_1 < p_1$.

It should be noted that the difference between the controllers of Equations (38) and (40) lies in the fact that the controller in Equation (40) has finite-time stability.

3. Controller design with FTSM-FTSM

The following controller (Equation (41)) for the system in Equation (10) is designed with FTSM-FTSM.

$$i_{qref} = \frac{2J}{3P_n\psi_f} \int_0^t \left(\frac{1}{J}B\dot{\omega}_m + \alpha_0\,x_2 + \frac{\beta_0\,q_0\,x_2\,x_1^{\frac{q_0}{p_0}-1}}{p_0} + \alpha_1\,s_1 + \beta_1\,s_1^{\frac{q_1}{p_1}} \right) d\tau \tag{41}$$

where $\alpha_i, \beta_i, \gamma_i > 0$, q_i, p_i are positive odd integers, and $q_i < p_i$, where $i = 0, 1$.

It should be noted that the difference between the controllers of Equations (38) and (41) lies in the fact that the controller in Equation (41) has finite-time stability.

4.3.2. Simulation Results and Discussion

In this section, we will compare the simulation results of the four different sliding modes: PTSM-PTSM, PTSM-LSM, FTSM-FTSM, and FTSM-LSM. To ensure a fair comparison, we have designed the relevant parameters of the conditions in Equations (19) and (26) for various sliding mode functions as $T_{p0} = 0.3$, $\mu_0 = 0.5$, $q_0/p_0 = 3/5$, $T_{p1} = 0.1$, $\mu_1 = 0.1$, and $q_1/p_1 = 3/5$.

The parameters of the four controllers (Equations (38)–(41)) used for simulation validation, which are calculated by considering the inequalities with an equal sign in Equations (19) and (26), are designed as $\alpha_0 = 33.33$, $\beta_0 = 8.33$, $\gamma_0 = 33.33$, $q_0/p_0 = 3/5$, $\alpha_1 = 100$, $\beta_1 = 5$, $\gamma_1 = 500$, $q_1/p_1 = 3/5$, and $c = 50$.

The reference speed N_{ref} is set to 1000 r/min in the simulations. The PMSM starts with only the inherent load T_{Lin} and the inherent viscous frictional coefficient B_{in} of the system. Then, the load increases suddenly to 1 N·m at 0.2 s.

From the comparative simulation results shown in Figure 7, the following conclusions can be drawn. In comparison to the speed regulation system controlled by four different sliding modes, PTSM-PTSM has a shorter settling time to reach the stable states, and all of them achieve the steady state without overshoot. When the load torque changes suddenly, the speed fluctuations under PTSM-PTSM are smallest, as illustrated in Figure 7a. In addition, both PTSM-LSM and FTSM-LSM share the same sliding surface, but they follow different phase trajectories, where PTSM-LSM achieves a higher convergence rate due to its utilization of the novel reaching law with PTSM. Similarly, both PTSM-PTSM and PTSM-LSM use the same reaching law, but they follow different phase trajectories, where PTSM-PTSM achieves a higher convergence rate due to its utilization of the novel sliding surface with PTSM.
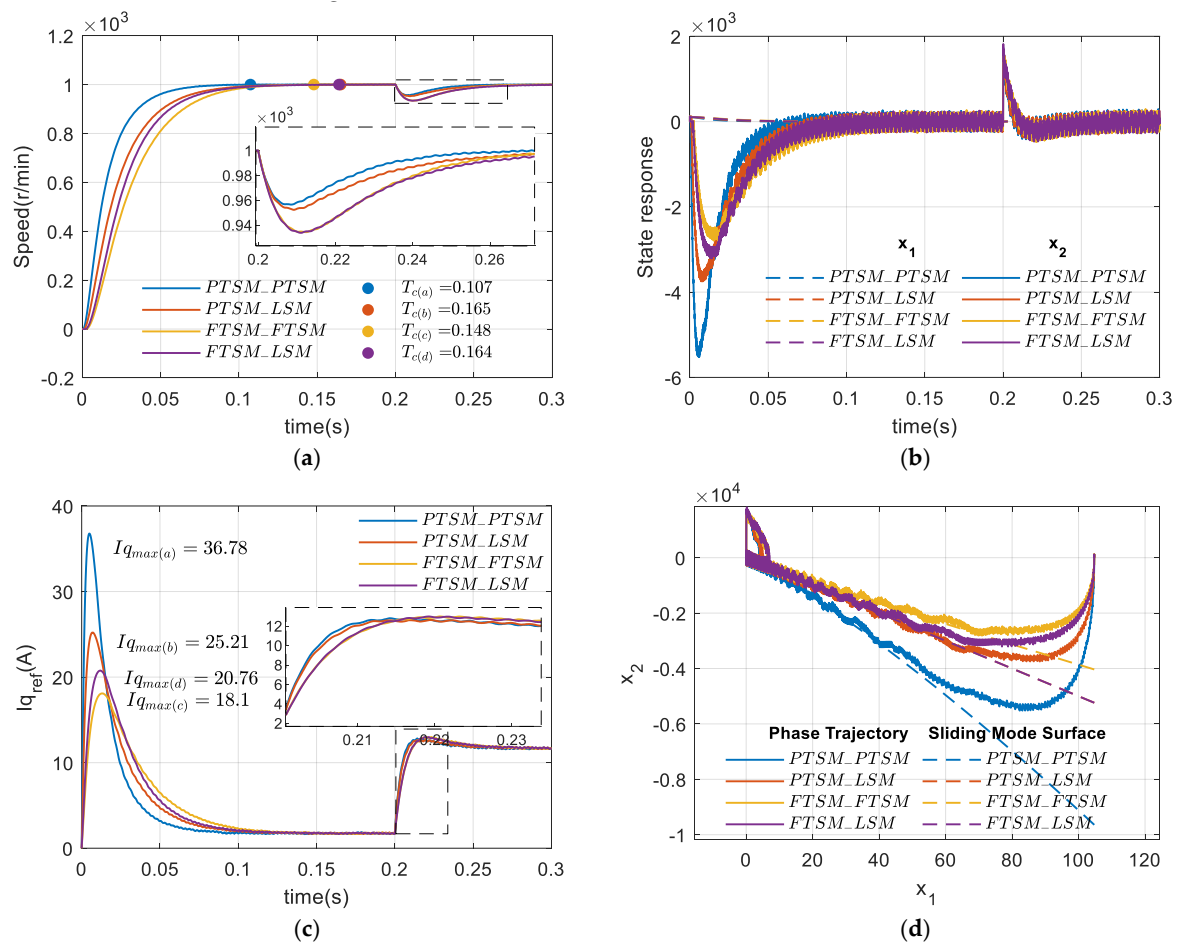
Figure 7. Comparative simulation under different sliding modes. (**a**) Speed tracking, (**b**) state responses, (**c**) control inputs, and (**d**) phase trajectories.

4.4. Comparative Experiments

To further validate the theoretical analysis and the proposed control method, an experiment platform for PMSM drive control shown in Figure 8 is established. The control system hardware is equipped with a 32-bit single-chip Aurix TriCore-based microcontroller TC275. In this section, the platform primarily aims to verify the dynamic response and robustness of the speed regulation system under PTSM-PTSM, PTSM-LSM, FTSM-FTSM, and FTSM-LSM.
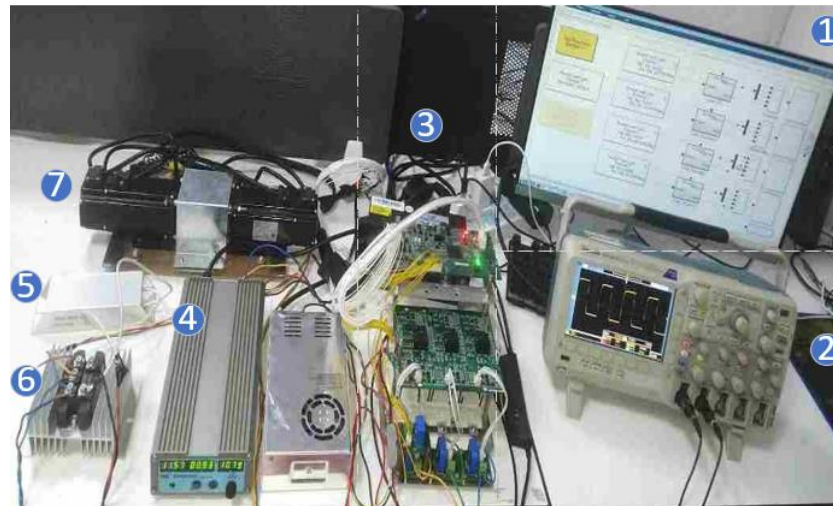
Figure 8. Experimental platform photograph. (1) Upper computer, (2) oscilloscope, (3) driver-board and Kvaser CAN, (4) DC-power, (5) resistive load, (6) rectifier, and (7) PMSM.

To ensure a fair comparison, we have designed the relevant parameters of the conditions in Equation (26) for various sliding mode functions as $T_{p0} = 1.2$, $\mu_0 = 0.6$, $q_0/p_0 = 3/5$, $T_{p1} = 3.5$, $\mu_1 = 0.01$, and $q_1/p_1 = 3/5$.

The parameters of the four controllers (Equations (38)–(41)) used for experiment validation are calculated by considering the inequalities with an equal sign in Equation (26) as $\alpha_0 = 8.333$, $\beta_0 = 2.5$, $\gamma_0 = 6.944$, $q_0/p_0 = 3/5$, $\alpha_1 = 2.857$, $\beta_1 = 0.014$, $\gamma_1 = 142.9$, $q_1/p_1 = 3/5$, and $c = 10$.

4. Dynamic responses test

The reference speed N_{ref} is set to 1000 r/min in the comparative experiments. The PMSM starts with only the inherent load T_{Lin} and the inherent viscous frictional coefficient B_{in} of the system. The parameters B_{in} and T_{Lin} are, respectively, designed as $B_{in} = 1.852 \times 10^{-4}$ N·m·s and $T_{Lin} = 6.658 \times 10^{-2}$ N·m.

5. Robust test

The second experiment is conducted to validate the robustness of the speed control system with four distinct control strategies. The PMSM is running at a steady state of 1000 r/min, and the load increases suddenly.

In motor-related tests, the electronic load often serves as a convenient substitute for simulating mechanical loads [48]. Thus, in this paper, a variable resistor is employed as the electronic load, as shown in Figure 8. Here, we set the external electronic load as a resistor with a resistance of $R_{ex} = 10\Omega$. Then, the parameters B_{ex} and T_{Lex} are, respectively, designed as $B_{ex} = 1.071 \times 10^{-3}$ N·m·s and $T_{Lex} = 5.399 \times 10^{-2}$ N·m.

The step response and load disturbance response of the four different control methods are shown in Figure 9; the reference speed can be tracked faster by PTSM-PTSM than others, and the states under PTSM-PTSM achieve the steady state without overshoot. When the load torque changes suddenly, PTSM-PTSM exhibits a minimal fluctuation in rotation speed.

From the control inputs of the comparative experimental results shown in Figure 10, we can draw the following conclusions. In the startup phase, a larger output of control input current can achieve faster convergence and a higher convergence rate. In the phase of load disturbance, PTSM-PTSM demonstrates the fastest performance in controlling the response speed of the input current. The specific convergence time of PTSM-PTSM is 35.2%

less than that of PTSM-LSM, 27.7% less than that of FTSM-FTSM, and 34.8% less than that of FTSM-LSM.
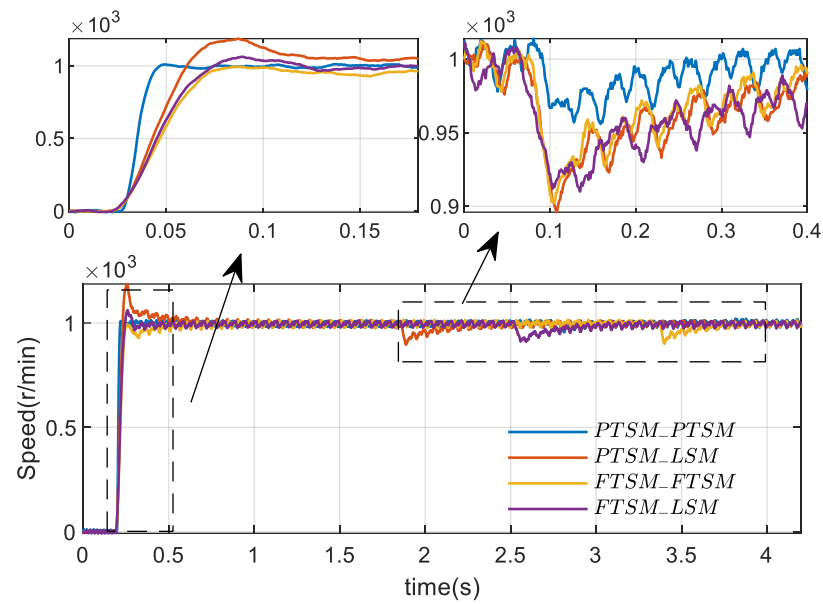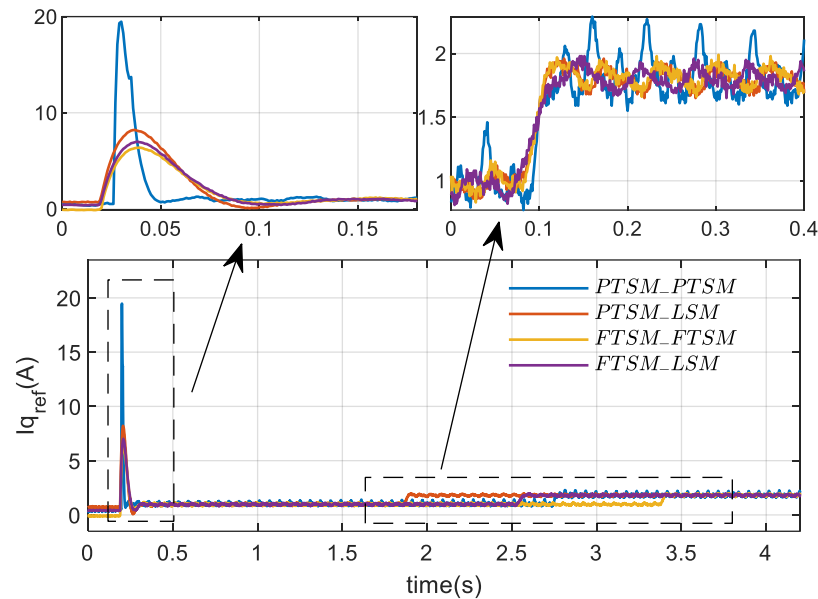

Figure 9. Speed tracking of comparative experiments.

Figure 10. Control inputs of comparative experiments.

5. Conclusions

In this paper, the SPTSM controller design with PTSM-PTSM for a second-order nonlinear SISO system is proposed, which has been investigated for the practical applications of the speed regulation system of PMSM. We focus on the impact of the relevant parameters of the SPTSM controller with PTSM-PTSM on the control effectiveness, which provides certain guidance for the selection of design parameters in controller design. The dynamic responsiveness and robustness of the system are validated through numerical simulations and experimental results. It has been observed that the robust SPTSM controller, which is designed with PTSM-PTSM, exhibits superior performance.

The main conclusions are as follows:

(1) This paper investigates the influence of several parameters in the second-order predefined-time terminal sliding mode (SPTSM), which significantly impact the system convergence effect and the convergence speed. The experimental results indicate that the conclusion offers certain guidance for the selection of parameters in controller design.

(2) By comparing the control input signals of four different control methods, both the simulation and the experimental results demonstrate that in the initial stage without an external load, a larger control input leads to a higher convergence rate of the system state. Among these methods, the PTSM-PTSM method shows a relatively faster convergence rate of the system state. Specifically, its experimental convergence time is 35.2% less than that of PTSM-LSM, 27.7% less than that of FTSM-FTSM, and 34.8% less than that of FTSM-LSM.

(3) When comparing the step responses and robust test with the load disturbance of four different control methods, the simulation and experimental results show that the following:

    (a) In the step responses stage, the control law of the speed regulation system of PMSM based on PTSM-PTSM has a faster convergence time than the other three control methods and does not exhibit overshoot during the process of converging to the stable state.

    (b) In the robust test with the load disturbance stage, the PTSM-PTSM method demonstrates better robustness than other three control methods.

It is worth highlighting that, according to our current understanding, this is the inaugural paper exploring the predefined-time stability of second-order nonlinear SISO systems, with a focus on the practical implications for the speed regulation system of a PMSM. Building on the current findings, our future work will focus on the following prioritized aspects:

(1) It is anticipated that the methodologies employed in this paper will be valuable in extending their application to other domains.

(2) The SPTSM, which is proposed in this paper, is capable of being extrapolated to high-order nonlinear control systems.

(3) The motor control system is governed by both the speed loop and the current loop. However, in this study, the current control system was not the primary focus. In the subsequent research, we will delve deeper into the control problems of the Multiple-Input Multiple-Output (MIMO) system based on SMC within the PMSM current loop system.

References

1. Jing, Z.; Yu, C.; Chen, G. Complex dynamics in a permanent-magnet synchronous motor model. *Chaos Solitons Fractals* **2004**, *22*, 831–848. [CrossRef]

2. Huang, G.; Wang, Q.; Zhang, N.; Jiang, C.; Ding, H. A Novel reaching law sliding mode control method of PMSM considering iron loss. *J. Frankl. Inst.* **2024**, *361*, 106857. [CrossRef]

3. Zheng, W.; Huang, R.; Luo, Y.; Chen, Y.; Wang, X.; Chen, Y. A Look-Up Table Based Fractional Order Composite Controller Synthesis Method for the PMSM Speed Servo System. *Fractal Fract.* **2022**, *6*, 47. [CrossRef]

4. Wang, B.; Wang, S.; Peng, Y.; Pi, Y.; Luo, Y. Design and High-Order Precision Numerical Implementation of Fractional-Order PI Controller for PMSM Speed System Based on FPGA. *Fractal Fract.* **2022**, *6*, 218. [CrossRef]

5. Niu, H.; Liu, L.; Jin, D.; Liu, S. High-Tracking-Precision Sensorless Control of PMSM System Based on Fractional Order Model Reference Adaptation. *Fractal Fract.* **2022**, *7*, 21. [CrossRef]

6. Wang, S.; Gan, H.; Luo, Y.; Luo, X.; Chen, Y. A Fractional-Order ADRC Architecture for a PMSM Position Servo System with Improved Disturbance Rejection. *Fractal Fract.* **2024**, *8*, 54. [CrossRef]

7. Moon, H.T.; Kim, H.S.; Youn, M.J. A discrete-time predictive current control for PMSM. *IEEE Trans. Power Electron.* **2003**, *18*, 464–472. [CrossRef]

8. Chen, C.-S.; Lin, W.-C. Self-adaptive interval type-2 neural fuzzy network control for PMLSM drives. *Expert Syst. Appl.* **2011**, *38*, 14679–14689. [CrossRef]

9. Ullah, A.; Pan, J.; Ullah, S.; Zhang, Z. Robust Speed Control of Permanent Magnet Synchronous Motor Drive System Using Sliding-Mode Disturbance Observer-Based Variable-Gain Fractional-Order Super-Twisting Sliding-Mode Control. *Fractal Fract.* **2024**, *8*, 368. [CrossRef]

10. Hou, H.; Yu, X.; Xu, L.; Rsetam, K.; Cao, Z. Finite-time continuous terminal sliding mode control of servo motor systems. *IEEE Trans. Ind. Electron.* **2020**, *67*, 5647–5656. [CrossRef]

11. Gil, J.; You, S.; Lee, Y.; Kim, W. Nonlinear sliding mode controller using disturbance observer for permanent magnet synchronous motors under disturbance. *Expert Syst. Appl.* **2023**, *214*, 119085. [CrossRef]

12. Yao, Y.; Li, Y.; Yin, Q. A novel method based on self-sensing motor drive system for misalignment detection. *Mech. Syst. Signal Proc.* **2019**, *116*, 217–229. [CrossRef]

13. Cao, Q.; Wei, D.Q. Dynamic surface sliding mode control of chaos in the fourth-order power system. *Chaos Solitons Fractals* **2023**, *170*, 113420. [CrossRef]

14. Chen, Y.; Wang, B.; Chen, Y.; Wang, Y. Sliding Mode Control for a Class of Nonlinear Fractional Order Systems with a Fractional Fixed-Time Reaching Law. *Fractal Fract.* **2022**, *6*, 678. [CrossRef]

15. Poursamad, A.; Markazi, A.H.D. Adaptive fuzzy sliding-mode control for multi-input multi-output chaotic systems. *Chaos Solitons Fractals* **2009**, *42*, 3100–3109. [CrossRef]

16. Jing, C.; Ma, X.; Zhang, K.; Wang, Y.; Yan, B.; Hui, Y. Actor-Critic Neural-Network-Based Fractional-Order Sliding Mode Control for Attitude Tracking of Spacecraft with Uncertainties and Actuator Faults. *Fractal Fract.* **2024**, *8*, 385. [CrossRef]

17. Mozayan, S.M.; Saad, M.; Vahedi, H.; Fortin-Blanchette, H.; Soltani, M. Sliding mode control of PMSG wind turbine based on enhanced exponential reaching law. *IEEE Trans. Ind. Electron.* **2016**, *63*, 6148–6159. [CrossRef]

18. Kim, K.-S.; Park, Y.; Oh, S.-H. Designing robust sliding hyperplanes for parametric uncertain systems: A Riccati approach. *Automatica* **2000**, *36*, 1041–1048. [CrossRef]

19. Nekoo, S.R. Digital implementation of a continuous-time nonlinear optimal controller: An experimental study with real-time computations. *ISA Trans.* **2020**, *101*, 346–357. [CrossRef] [PubMed]

20. Wang, J.; Chen, M.Z.Q.; Zhang, L. Observer-based discrete-time sliding mode control for systems with unmatched uncertainties. *J. Frankl. Inst.* **2021**, *358*, 8470–8484. [CrossRef]

21. Wu, Y.; Man, Z.; Yu, X. Terminal sliding mode control design for uncertain dynamic systems. *Syst. Control. Lett.* **1998**, *34*, 281–287. [CrossRef]

22. Wang, C. Adaptive Terminal Sliding-Mode Synchronization Control with Chattering Elimination for a Fractional-Order Chaotic System. *Fractal Fract.* **2024**, *8*, 188. [CrossRef]

23. Feng, Y.; Yu, X.; Han, F. On nonsingular terminal sliding-mode control of nonlinear systems. *Automatica* **2013**, *49*, 1715–1722. [CrossRef]

24. Jiang, J.; Chen, H.; Cao, D.; Guirao, J.L.G. The global sliding mode tracking control for a class of variable order fractional differential systems. *Chaos Solitons Fractals* **2022**, *154*, 111674. [CrossRef]

25. Lu, S.; Wang, X.; Li, Y. Adaptive neural network finite-time command filtered tracking control of fractional-order permanent magnet synchronous motor with input saturation. *J. Frankl. Inst.* **2020**, *357*, 13707–13733. [CrossRef]

26. Jia, T.; Chen, X.; He, L.; Zhao, F.; Qiu, J. Finite-Time Synchronization of Uncertain Fractional-Order Delayed Memristive Neural Networks via Adaptive Sliding Mode Control and Its Application. *Fractal Fract.* **2022**, *6*, 502. [CrossRef]

27. Ding, L.; Xia, T.; Ma, R.; Liang, D.; Lu, M.; Wu, H. Enhanced Impedance Control of Cable-Driven Unmanned Aerial Manipulators Using Fractional-Order Nonsingular Terminal Sliding Mode Control with Disturbance Observer Integration. *Fractal Fract.* **2024**, *8*, 579. [CrossRef]

28. Labbadi, M.; Boubaker, S.; Djemai, M.; Mekni, S.K.; Bekrar, A. Fixed-Time Fractional-Order Global Sliding Mode Control for Nonholonomic Mobile Robot Systems under External Disturbances. *Fractal Fract.* **2022**, *6*, 177. [CrossRef]

29. Shao, K.-Y.; Feng, A.; Wang, T.-T. Fixed-Time Sliding Mode Synchronization of Uncertain Fractional-Order Hyperchaotic Systems by Using a Novel Non-Singleton-Interval Type-2 Probabilistic Fuzzy Neural Network. *Fractal Fract.* **2023**, *7*, 247. [CrossRef]

30. Benaddy, A.; Labbadi, M.; Elyaalaoui, K.; Bouzi, M. Fixed-Time Fractional-Order Sliding Mode Control for UAVs under External Disturbances. *Fractal Fract.* **2023**, *7*, 775. [CrossRef]

31. Xue, H.; Liu, X. A novel fast terminal sliding mode with predefined-time synchronization. *Chaos Solitons Fractals* **2023**, *175*, 114049. [CrossRef]

32. Anguiano-Gijón, C.A.; Muñoz-Vázquez, A.J.; Sánchez-Torres, J.D.; Romero-Galván, G.; Martínez-Reyes, F. On predefined-time synchronisation of chaotic systems. *Chaos Solitons Fractals* **2019**, *122*, 172–178. [CrossRef]

33. Munoz-Vazquez, A.J.; Sanchez-Torres, J.D.; Jimenez-Rodriguez, E.; Loukianov, A.G. Predefined-time robust stabilization of robotic manipulators. *IEEE-ASME Trans Mechatron.* **2019**, *24*, 1033–1040. [CrossRef]

34. Zhang, R.; Xu, B.; Zhao, W. Finite-time prescribed performance control of MEMS gyroscopes. *Nonlinear Dyn.* **2020**, *101*, 2223–2234. [CrossRef]

35. Song, S.; Xing, L.; Song, X.; Tejado, I. Event-Triggered Fuzzy Adaptive Predefined-Time Control for Fractional-Order Nonlinear Systems with Time-Varying Deferred Constraints and Its Application. *Fractal Fract.* **2024**, *8*, 613. [CrossRef]

36. Ni, J.-K.; Liu, C.-X.; Liu, K.; Liu, L. Finite-time sliding mode synchronization of chaotic systems. *Chin. Phys. B* **2014**, *23*, 100504. [CrossRef]

37. Zhang, M.; Zang, H.; Bai, L. A new predefined-time sliding mode control scheme for synchronizing chaotic systems. *Chaos Solitons Fractals* **2022**, *164*, 112745. [CrossRef]

38. Zhang, S.; Wang, C.; Zhang, H.; Ma, P.; Li, X. Dynamic analysis and bursting oscillation control of fractional-order permanent magnet synchronous motor system. *Chaos Solitons Fractals* **2022**, *156*, 111809. [CrossRef]

39. Sánchez-Torres, J.D.; Gómez-Gutiérrez, D.; López, E.; Loukianov, A.G. A class of predefined-time stable dynamical systems. *IMA J. Math. Control Inf.* **2018**, *35*, i1–i29. [CrossRef]

40. Abudusaimaiti, M.; Abdurahman, A.; Jiang, H.; Hu, C. Fixed/predefined-time synchronization of fuzzy neural networks with stochastic perturbations. *Chaos Solitons Fractals* **2022**, *154*, 111596. [CrossRef]

41. Chen, C.; Mi, L.; Liu, Z.; Qiu, B.; Zhao, H.; Xu, L. Predefined-time synchronization of competitive neural networks. *Neural Netw.* **2021**, *142*, 492–499. [CrossRef] [PubMed]

42. Salle, J.L.; Lefschetz, S.; Alverson, R.C. *Stability by Liapunov's Direct Method With Applications*; Academic Press: New York, NY, USA, 1961.

43. Huang, P.; Zhang, Z.; Gao, Y. Amplitude-saturated control of underactuated double-pendulum tower cranes: Design and experiments. *Mech. Syst. Signal Proc.* **2025**, *228*, 112419. [CrossRef]

44. Gallegos, J.A.; Duarte-Mermoud, M.A. On the Lyapunov theory for fractional order systems. *Appl. Math. Comput.* **2016**, *287*, 161–170. [CrossRef]

45. Yu, X.; Zhihong, M. Fast terminal sliding-mode control design for nonlinear dynamical systems. *IEEE Trans. Circuits Syst. I-Regul. Pap.* **2002**, *49*, 261–264. [CrossRef]

46. Wang, Y.; Feng, Y.; Zhang, X.; Liang, J. A new reaching law for antidisturbance sliding-mode control of PMSM speed regulation system. *IEEE Trans. Power Electron.* **2020**, *35*, 4117–4126. [CrossRef]

47. Liu, J. *Sliding Mode Control Using MATLAB*; Elsevier Inc.: Amsterdam, The Netherlands; Tsinghua University: Beijing, China, 2017; p. 346.

48. Arellano-Padilla, J.; Asher, G.M.; Sumner, M. Control of an AC Dynamometer for Dynamic Emulation of Mechanical Loads With Stiff and Flexible Shafts. *IEEE Trans. Ind. Electron.* **2006**, *53*, 1250–1260. [CrossRef]